Temperature dependence of the exciton dynamics in DCM2:Alq_{3}

Xiao Liu, Yifan Zhang, and Stephen R. Forrest

Phys. Rev. B **90**, 085201 — Published 7 August 2014

DOI: 10.1103/PhysRevB.90.085201

Temperature Dependence of the Exciton Dynamics in DCM2:Alq_3

Xiao Liu[1], Yifan Zhang[2], Stephen R. Forrest[1,2,3]

[1]*Department of Electrical Engineering and Computer Science, University of Michigan*

[2]*Department of Physics, University of Michigan*

[3]*Departments of Material Science and Engineering, University of Michigan*

Ann Arbor, MI 48109, USA

Abstract

We study the temperature dependence of the triplet and singlet exciton dynamics in the archetype small molecule fluorescent guest-host system, *tris*(8-hydroxyquinolinato) aluminum (Alq_3) doped with 4-(dicyanomethylene)-2-methyl-6-julolidyl-9-enyl-4H-pyran (DCM2). We develop a comprehensive model of the exciton dynamics, and use it to fit the transient photoluminescence under different pulsed optical pumping in the temperature range of 80 K< *T*< 295 K. The triplet decay has a significantly different temperature dependence than that of singlets. From 295K to 80K, the triplet-triplet annihilation (TTA) rate decreases by two orders of magnitude, whereas the singlet-triplet annihilation rate decreases by <50% primarily a result of the different energy transfer mechanisms of singlets and triplets. The temperature dependence of TTA rate reveals two regimes separated by a transition at 180K from Marcus to Miller-Abrahams transfer. This work deepens our understanding of exciton dynamics and energy transfer in small molecule organic materials.

I. Introduction

Excitons, or molecular excited states, play a central role in the properties of organic (i.e. excitonic) materials [1]. Understanding and ultimately controlling their dynamical properties is essential to quantifying the nature of optoelectronic organic thin films, and in optimizing the characteristics of devices in which they are employed.

During their lifetime, excitons can migrate within a material via a succession of energy transfer steps mediated by either Dexter exchange [2] or electrostatic Förster interactions [3]. While spin anti-symmetric singlet excitons favor transport via Förster resonant energy transfer (FRET), spin-forbidden symmetric triplet excitons diffuse primarily via hopping from the donor to acceptor molecules, as described by Dexter [2]. With an adequate understanding of these properties, management of singlet and triplet energy transfer can, for example, lead to high efficiency white organic light emitting diodes (OLEDs) [4], or determine the rate of triplet-triplet (TTA) and/or singlet-triplet annihilation (STA) in fluorescent OLEDs [5-9]. Furthermore, it has been shown that exciton management in organic semiconductor lasers can mitigate triplet-induced losses to result in quasi-continuous wave lasing [10].

The temperature dependence of the exciton dynamics provides insight into the mechanisms that govern both diffusion and annihilation of excitons. Previous work has reported on the temperature dependence of triplet exciton transport in benzophenone glass [11], intra-chain triplet diffusion and TTA in both solution and bulk films of a poly(fluorene) derivative [12], and triplet energy transfer in conjugated polymers [13-15]. While the dynamics of singlet excitons *vs*. temperature were explored in neat Alq_3 [16], to our knowledge the temperature dependence of emissive singlet and non-emissive triplet states has yet to be systematically

studied in an efficient small molecule fluorescent guest-host system. In this work, we explore the temperature dependence of the singlet and triplet dynamics in the archetype fluorescent guest-host system comprised of *tris* (8-hydroxyquinolinato) aluminum (Alq_3) doped with the red emitting 4-(dicyanomethylene)-2-methyl-6-julolidyl-9-enyl-4H-pyran (DCM2).

This paper is organized as follows: In Sec. II, we develop a model describing the singlet and triplet dynamics in fluorescent guest-host systems. Section III provides experimental details. Results of transient photoluminescence (PL) measurements under pulsed optical pumping, and fits to the model are provided in Sec. IV where significantly different temperature dependences for singlets and triplets are described. The phenomena are discussed in terms of theoretical models in Sec. V, and in Sec. VI we present conclusions.

II. Theory

By the appropriate choice of illumination wavelength, singlets are directly generated on the host followed by their Förster transfer to the guest. Triplets can also be generated on the host through intersystem crossing of singlets. Host triplets then transfer to the guest via hopping (i.e. via a Dexter process). The singlet (S), host triplet (T_h), and guest triplet (T_g) densities as functions of time, t, are described using [10]:

$$\frac{dS}{dt} = \frac{\eta I}{e_p d} - k_S S - k_{ISC} S - k_{ST} S T_g \,, \tag{1}$$

$$\frac{dT_h}{dt} = k_{ISC} S - k_{hg} exp\left(-\frac{2}{L}\sqrt[3]{\frac{1}{N_0 - T_g}} \right) T_h - k_{T(h)} T_h - \frac{1}{2} k_{TT(h)} T_h^2 , \tag{2}$$

$$\frac{dT_g}{dt} = k_{hg} exp\left(-\frac{2}{L}\sqrt[3]{\frac{1}{N_0 - T_g}} \right) T_h - k_{T(g)} T_g - \frac{1}{2} k_{TT(g)} T_g^2 . \quad (3)$$

Here I is the optical pump power density, η is the fraction of the pump power absorbed by the film, e_p is the photon energy, and d is the film thickness. Singlet decay processes are described by several rates, including natural decay (k_S), intersystem crossing (k_{ISC}), and annihilation between a guest singlet and triplet (k_{ST}). We neglect guest singlet and host triplet interactions since the large host triplet TTA rate results in a relatively low host triplet density. For example, a TTA rate of $k_{TT} = 10^{-12}$ cm^3·s^{-1} has been reported for Alq_3 at room temperature [17], which is three orders of magnitude larger than the rate of TTA on the relatively low density of DCM2 dopant molecules. This assumption will be discussed further in Sec. IV. Also, N_0 is the guest triplet saturation density [10], k_{hg} is the pre-factor for host-guest Dexter transfer, and L is the effective localization radius of the exciton on the molecule (~1 nm) [10]. The triplet decay rate includes the triplet natural decay (k_T) and TTA.

Guest triplet natural decay, annihilation on the guest, and triplet natural decay on the host (described by $k_{T(g)}$, $k_{TT(g)}$, and $k_{T(h)}$, respectively) are neglected in modeling the turn-on transient of the PL signal due to their relatively minor influence during the build-up of the triplet population. Following the pump pulse, only guest triplet dynamics are considered due to the fast decay of singlets and host triplets [17], in which case Eq. (3) becomes:

$$\frac{dT_g}{dt} = -k_{T(g)} T_g - \frac{1}{2} k_{TT(g)} T_g^2 . \quad (4)$$

Based on this theory, we analyze: (i) the singlet evolution in the presence of host and guest triplet annihilation model described in Eq. (1) – (3) by measuring the PL turn-on transient

using a >20μs pulse; (ii) the singlet decay by measuring the PL response to a short (~1ns) pulse; (iii) the triplet density decay described in Eq. (4) by measuring its transient absorption following the turn-off of pump pulse.

III. Experimental

Organic films were deposited by vacuum thermal evaporation at a base pressure of 8×10^{-7} torr. Films of DCM2 co-deposited with Alq_3 at a 3% vol. concentration were grown on a Si substrate to a thickness of 50 nm for use in the PL turn-on transient and singlet decay measurements. 200 nm thick 3%, 8%, and 15% vol. DCM2:Alq_3 and undoped Alq_3 films were grown on 2-μm-thick SiO_2-on-Si substrates forming an air-organic-SiO_2 slab waveguide for pump-probe guest triplet density measurements [17]. Temperature was controlled in the range between 295 K and 80 K using a closed-cycle cryostat (Janis SHI 4-5).

For PL turn-on transient measurements, the sample was pumped using a laser diode at a wavelength of $\lambda = 405$ nm (Nichia NDV7116), whose beam power density was 15 W/cm^2 to 150 W/cm^2 focused on a 490 μm × 900 μm spot on the film. The laser was driven using 30 μs pulses at a 1 Hz repetition rate (HP 8114A pulse generator). The PL transients were measured using a photodiode (FPD 510-FV) and an oscilloscope. Singlet lifetimes were measured using a N_2 laser for pump (λ = 337 nm, pulse width = 1.5 ns) and a streak camera (Hamamatsu C4334) with a time resolution of 40 ps.

Triplet exciton density decay following the pump pulse was determined by pump-probe triplet absorption [17]. The $\lambda = 405$ nm laser diode was used as the pump with a power of 680 mW and spot size of 2900 μm × 1500 μm positioned adjacent to a cleaved edge of the substrate.

The pulse conditions were the same as above. The probe (N_2 laser) beam was focused to a 1500 μm × 390 μm spot separated by 1600 μm from the pump spot, and was delayed by 1 μs to 800 ms following the pump. Photons generated by the probe were waveguided through the triplet populated region created by the pump, and emitted from the cleaved edge where both spectrally and temporally resolved emission were measured using a streak camera. Measurement of the attenuated edge emission intensity *vs.* the length of the pump region yields the triplet absorption coefficient, α at each wavelength. The average triplet absorption is calculated between wavelengths from 520 nm –640 nm for Alq_3 and 640 nm –750 nm for DCM2:Alq_3.

IV. Results

Photoluminescence turn-on transients for a 3% vol. DCM2:Alq_3 film at four different power densities at room temperature (295 K) are shown in Fig. 1(a). Figure 1(b) shows the PL vs. temperature for a power density of 58mW/cm^2. From these data, the PL turn-on transients show only minor temperature dependence. The PL data at four different power densities are fit using Eqs. (1) - (3) with N_0, k_{ST}, and k_{ISC} as parameters, which are indicated by the solid lines. Parameters have no systematic dependence on power over the range explored. Note that k_S at each temperature is obtained from the singlet lifetime measurement, and $k_{TT(h)}$ is measured using pump-probe triplet absorption where the sample is an undoped, 200 nm thick Alq_3 film on the SiO_2-on-Si substrate. Finally, $k_{hg} = 4 \times 10^{10}$ s^{-1} is obtained from Ref.[10]. Figure 2 shows the result of fits that yield N_0, k_{ST}, and k_{ISC} from the PL transients in Fig. 1. The STA rate, k_{ST}, decreases by <50% when the temperature is decreased from room temperature to 80 K. In

contrast, the intersystem crossing rate, k_{ISC}, remains relatively constant over this same temperature range while the guest triplet saturation density, N_0, increases slightly.

Figure 3 shows the transient PL response following a 1.5 ns pump pulse for the sample in Fig. 1. We assume only the singlet density is important given the low intersystem crossing rate of $\sim 10^7$ s^{-1}. The singlet lifetime is calculated by deconvolving the temporal profiles of the laser pulse and PL for a pump intensity of 4 $\mu J/cm^2$, where singlet-singlet annihilation is neglected. Table I provides the singlet lifetimes inferred from the fits.

The edge emission at room temperature obtained in the guest triplet absorption measurement is shown in Fig. 4(a). Figure 4(b) shows a minor change of guest triplet absorption across the spectral region of the probe. For simplicity of analysis, the average triplet absorption coefficient is converted to the triplet density when divided by the DCM2 guest triplet absorption cross section of 4×10^{-17} cm^2 [10]. The normalized guest triplet density in DCM2:Alq_3 *vs*. temperature and time following the pump pulse is shown in Fig. 5. Equation (4) is used to fit the data (solid lines). The triplet density at 80K takes ten times longer to decrease to 10% of its original value compared to room temperature. Comparison of Figs. 3 and 5 indicates that the triplet decay is temperature dependent from 80 K to 295 K, whereas singlet decay is not.

We can obtain the host triplet density when applying the same method to undoped Alq_3 film, which is shown in the inset of Fig. 5. The results of the fits to the data are provided in Table II. Our observations indicate that TTA rate of host triplets is several orders of magnitude larger than that of guest triplets. Following the pump pulse, fast decay of host triplets results in their limited contribution to the long-lived guest triplets decay.

Table III and Figure 6(a) show the triplet lifetime and k_{TT} obtained from the fits in Fig. 5, respectively. The temperature dependence of the k_{TT} and triplet natural lifetime in films with 3%, 8%, and 15% vol. doping concentration follows similar trends, as indicated in Figs. 6b, 6c and Table III. For 3% vol. DCM2:Alq_3, $k_{TT} = (1.6 \pm 0.1) \times 10^{-15}$ $cm^3 \cdot s^{-1}$ at room temperature, which is close to $k_{TT} = 1 \times 10^{-15}$ $cm^3 \cdot s^{-1}$ previously reported for the DCM:Alq_3 system [10, 17]. Reducing the temperature to 80 K results in a 20 times reduction to $k_{TT} = 5.1 \times 10^{-17}$ $cm^3 \cdot s^{-1}$. This is in striking contrast to the temperature dependence of k_{ST} in Fig. 2. When log (k_{TT}) vs. 1000/T is plotted in Fig. 6, two distinct slopes with a transition temperature $T_{trans} \approx 180$K are observed.

V. Discussion

In fluorescent systems, the natural decay rate (k_T) of non-emissive triplets has a limited contribution to the triplet density. The temperature dependence of the triplet density is therefore determined by the temperature dependence of TTA. Now [18]:

$$k_{TT} = 8\pi \cdot R_Q \cdot D_T, \tag{5}$$

where D_T is the triplet diffusivity and R_Q is the triplet interaction radius. Since R_Q is temperature independent, D_T provides the temperature dependence of k_{TT}.

The temperature dependent triplet diffusivity corresponding to k_{TT} in Fig. 6 reveals two separate temperature activated regimes indicative of two different triplet energy transfer mechanisms. At temperatures above the transition between rates (i.e. $T > T_{trans} \approx 180$K), triplet diffusion is described by Marcus transfer [14]. During Dexter transfer, the simultaneous exchange of two electrons occurs between the highest occupied and lowest unoccupied molecular orbital levels of adjacent donor and acceptor molecules, which undergo a

configuration change during transfer. During Marcus transfer, multiple phonons are required to overcome the energy barriers separating the sites (denoted by an activation energy E_a) and the differences in the site energies [14, 15]. The site energy difference itself is attributed to morphological disorder in the amorphous thin film, where the site-specific orientation of dipoles between molecules leads to an inhomogeneously broadened density of states (DOS). The half width of the Gaussian DOS distribution (σ) corresponds to the degree of orientational order; narrow distributions reflect a more ordered environment.

Temperatures below the transition (i.e. $T < T_{trans}$), multi-phonon Marcus transfer is less probable. In this case, phonon-assisted tunneling between energetically disordered sites described by Miller-Abrahams transfer theory is more appropriate [14, 19]. Moreover, dispersive triplet diffusion is prevalent at low temperatures [11, 20, 21]. Following excitation, triplets relax towards the low-energy tail of the DOS, resulting in a hopping towards acceptor sites at lower energy [11, 13]. Decreasing the temperature slows hopping, thereby reducing D_T.

The respective diffusivity, D_T (proportional to the triplet energy transfer rate, W) *vs.* temperature (T) above and below T_{trans} is thus described by [14, 15]:

$$D_T \propto W = \frac{J_0^2}{\hbar}\sqrt{\frac{\pi}{4E_a k_B T}}\exp(-2\frac{a}{L})\exp(-\frac{E_a}{k_B T}-\frac{1}{8}(\frac{\sigma}{k_B T})^2), \quad T>T_{trans} \tag{7}$$

$$D_T \propto W = \gamma_0\exp(-2\frac{a}{L})\exp\left[-\frac{1}{2}(\frac{\sigma}{k_B T})^2\right], \quad T<T_{trans} \tag{8}$$

where k_B is Boltzmann's constant, α is the average distance between donor and acceptor sites, L is the effective localization radius of triplets, J_0 is the electronic coupling integral prefactor, and γ_0 is the characteristic frequency of the phonon.

In Fig. 6, we fit the data above (Marcus) and below (Miller-Abrahams) T_{trans} to Eqs. (7) and (8), respectively at three different DCM2 doping concentrations. The σ from three fits are identical within the experimental confidence limits, with an average of σ = 7.8 ± 0.9 meV. Energetic disorder (σ) of some organic systems can be large, for example, for poly[methyl(phenyl)silylene] (PMPSi), σ = 89 meV; for poly[biphenylyl(methyl)silylene] (PBPMSi), σ = 94 meV [22]; and for poly(2,7-(9,9-bis(2-ethylhexyl)fluorene)) (PF2/6), σ = 40meV [12]. In contrast, DCM2:Alq_3 films possess considerably less disorder as reflected in their narrow DOS. The fit of Eq. (8) to the data yields a ratio of $\exp(-\frac{2a_{3\%}}{L}) : \exp(-\frac{2a_{8\%}}{L}) : \exp(-\frac{2a_{15\%}}{L}) \approx$ 1.7:1.4:1, which indicates that 15% vol. doping concentration has the largest average distance between the neighboring triplets. This is likely due to concentration quenching, where a large DCM2 concentration leads to a low quantum yield and large separation of guest triplets [23].

Activation energies of E_a = 105 ± 8 meV, 124 ± 12 meV, 131 ± 13 meV are obtained from the fit for 3%, 8%, and 15% vol. DCM2:Alq_3, respectively. The electron coupling integral $J = J_0 \exp(-\frac{a}{L})$ between the neighboring sites has a measured ratio of $J_{3\%} : J_{8\%} : J_{15\%} \approx$ 1:1.7:1.8. This suggests that higher guest concentrations lead to an increased overlap of the donor and acceptor electronic wave functions, as expected.

The temperature dependence above and below T_{trans} is dominated by E_a and σ, respectively. A low ratio of σ/E_a leads to a more obvious distinction in slopes between the two regimes. Small disorder, and thus a large distinction between σ and E_a increases the transition temperature [14]. In our case, a low disorder results in a transition at $T\approx$180K which is higher

than reported for other systems. For example, the Pt-polymer (poly[trans(bis(tributylphosphine))Pt(1,4) phenylenediethynylene) transition occurs at 80K [15], and for poly[2-methyl-5-(3',7'-dimethyloctyloxy)-*p*-phenylenevinylene] (MDMO-PPV), the temperature is 150K [13].

Thermal activation of exciton transport is observed only if the hopping occurs between nearest neighbors coupled by the exchange interaction. Therefore, it is a dominant factor governing triplet rather than singlet transport. Förster transfer of singlets occurs by long range electrostatic interactions leading to its temperature independence [21]. In our measurements, the PL response of the films (Figs. 1 and 3) is dominated by singlet dynamics, and hence is only weakly dependent on temperature. Now, the singlet-triplet annihilation rate is [18, 24]:

$$k_{ST} = 0.676 \times 4\pi \left(\frac{R_{ST}^{\ 6}}{\tau_S \phi_F}\right)^{1/4} D_{ST}^{3/4}, \qquad (9)$$

where D_{ST} is the combined diffusivity of the singlet and triplet states, R_{ST} is their interaction radius, τ_S is the singlet lifetime, and ϕ_F is the FRET efficiency. The singlet diffusivity (D_S) is usually much larger than that of triplets (D_T): for example, D_S is between 0.1 and 1 cm^2/s [25], while $D_T = 2 \times 10^{-4}$ cm^2/s in anthracene [26]. Thus we expect D_S to dominate D_{ST} in the DCM2:Alq_3 system, leading to the weak temperature dependence observed for k_{ST}.

VI. Conclusions

We have observed significantly different temperature dependences of the singlet and triplet density dynamics in the archetype small molecule fluorescent organic system comprised of Alq_3 doped with DCM2. From 295K to 80K, the large temperature dependence of the non-

emissive guest triplet diffusivity results in a decrease in the triplet-triplet annihilation rate of ~20 times. The two temperature regimes observed for k_{TT} reveal that the diffusivity of triplets is determined by the dominance of thermally activated multi-phonon Marcus transfer at high temperatures, and Miller-Abrahams single phonon assisted hopping at low temperatures. Förster transfer leads to a weakly temperature dependent singlet diffusivity, resulting in a similarly weak temperature dependent singlet-triplet annihilation process. This suggests that singlet and triplet diffusion can be separately controlled due to their different energy transfer mechanisms. For example, the triplet is localized at low temperature without affecting the singlet dynamics, eventually allowing for improved management of exciton energy transport in luminescent materials systems.

Acknowledgments

We are grateful to the Center for Energy Nanoscience, an Energy Frontier Research Center at the University of Southern California supported by the U.S. Department of Energy (Grant no. DE-SC0001013; XL experiment, analysis; YZ analysis), and Universal Display Corp. (SRF, analysis, experimental concept) for partial support of this work. Also, SRF would like to thank the Technion, Israel Institute of Technology for support from a Lady Davis Visiting Professorship.

References

[1] M. Pope, and C. Swenberg, *Electronic Processes in Organic Crystals and Polymers* (Oxford University Press, New York, NY, 1999), 2nd edn.

[2] D. L. Dexter, The Journal of Chemical Physics **21**, 836 (1953).

[3] T. Förster, Ann. Physics **437**, 55 (1948).

[4] Y. Sun, N. C. Giebink, H. Kanno, B. Ma, M. E. Thompson, and S. R. Forrest, Nature **440**, 908 (2006).

[5] Y. Zhang, and S. R. Forrest, Physical Review Letters **108**, 267404 (2012).

[6] B. H. Wallikewitz, D. Kabra, S. Gélinas, and R. H. Friend, Physical Review B **85**, 045209 (2012).

[7] Y. Luo, and H. Aziz, Advanced Functional Materials **20**, 1285 (2010).

[8] D. Kasemann, R. Brückner, H. Fröb, and K. Leo, Physical Review B **84**, 115208 (2011).

[9] Y. Zhang, M. Whited, M. E. Thompson, and S. R. Forrest, Chemical Physics Letters **495**, 161 (2010).

[10] Y. Zhang, and S. R. Forrest, Physical Review B **84**, 241301(R) (2011).

[11] R. Richert, and H. Ba□ssler, The Journal of Chemical Physics **84**, 3567 (1986).

[12] D. Hertel, H. Ba□ssler, R. Guentner, and U. Scherf, The Journal of Chemical Physics **115**, 10007 (2001).

[13] O. V. Mikhnenko, F. Cordella, A. B. Sieval, J. C. Hummelen, P. W. M. Blom, and M. A. Loi, The Journal of Physical Chemistry. B **112**, 11601 (2008).

[14] I. Fishchuk, A. Kadashchuk, L. Sudha Devi, P. Heremans, H. Bässler, and A. Köhler, Physical Review B **78**, 045211 (2008).

[15] L. Sudha Devi, M. Al-Suti, C. Dosche, M. Khan, R. Friend, and A. Köhler, Physical Review B **78**, 045210 (2008).

[16] R. Priestley, A. D. Walser, and R. Dorsinville, Optics Communications **158**, 93 (1998).

[17] M. Lehnhardt, T. Riedl, T. Rabe, and W. Kowalsky, Organic Electronics **12**, 486 (2011).

[18] S. Chandrasekhar, Reviews of Modern Physics **15** (1943).

[19] A. Miller, and E. Abrahams, Phycial Review **120**, 745 (1960).

[20] B. Movaghar, M. Grünewald, B. Ries, H. Bassler, and D. Würtz, Physical Review B **33**, 5545 (1986).

[21] A. Köhler, and H. Bässler, Materials Science and Engineering R **66**, 71 (2009).

[22] I. Fishchuk, A. Kadashchuk, H. Bässler, and S. Nešpůrek, Physical Review B **67**, 224303 (2003).

[23] C. W. Tang, S. A. VanSlyke, and C. H. Chen, Journal of Applied Physics **65** (1989).

[24] M. Yokota, and O. Tanimoto, Journal of the Physical Society of Japan **22**, 779 (1967).

[25] Y. Takahashi, and M. Tomura, Journal of the Physical Society of Japan **31**, 1100 (1971).

[26] V. Ern, P. Avakian, and R. Merrifield, Physical Review **148**, 862 (1966).

TABLE I.

Singlet lifetime of a 3% vol. DCM2:Alq_3 film *vs.* temperature.

Temperature (K)	295	270	240	210	180	150	120	80
Lifetime (ns)	1.14 ±0.02	1.21 ±0.01	1.33 ±0.02	1.38 ±0.03	1.30 ±0.02	1.26 ±0.02	1.37 ±0.03	1.28 ±0.02

TABLE II.

Triplet-triplet annihilation rate *vs.* temperature for Alq_3.

Temperature (K)	295	270	240	210	180	150	120	100	80
k_{TT}	1.9	1.1	0.81	0.27	0.22	0.079	0.029	0.0081	0.0018
($\times 10^{-12}$ cm^3/s)	±0.27	±0.25	±0.39	±0.22	±0.26	±0.034	±0.027	±0.0069	±0.0043

TABLE III.

Guest triplet natural lifetime *vs.* temperature in 3%, 8%, and 15% vol. DCM2:Alq_3 films

Temperature (K)	295	270	240	210	180	150	120	100	80
	3% vol.								
	50.0	120.2	122.7	150.7	154.1	170.5	194.0	177.3	215.1
	±11.5	±22.3	±20.7	±30.8	±16.4	±17.5	±12.6	±12.3	±14.8
	8% vol.								
Lifetime (ms)	73.1	107.0	137.5	141.3	136.5	150.1	175.3	167.2	178.0
	±11.3	±24.5	±18.7	±10.1	±7.8	±8.9	±8.1	±11.1	±14.3
	15% vol.								
	44.9	101.4	126.5	139.5	168.5	182.7	172.8	231.9	230.5
	±7.5	±16.8	±19.1	±8.2	±6.9	±13.0	±11.0	±19.5	±21.3
Average	56.0	109.5	128.9	143.8	153.0	167.8	180.7	192.1	207.9

Figure captions

Figure 1. (a) Photoluminescence (PL) turn-on transient for a 3% vol. DCM2:Alq_3 film at T=295K under four different power densities. The data are normalized to the peak PL at 147 W/cm^2. Solid lines are fits to the annihilation model in eq. (1) – (3). (b) Temperature dependence of the time resolved PL at 58W/cm^2. The PL transient decay slightly slows down as the temperature decreases.

Figure 2. Temperature dependence of the rates of singlet-triplet annihilation, k_{ST}, intersystem crossing, k_{ISC}, and the guest triplet saturation density N_0 for 3% vol. DCM2:Alq_3.

Figure 3. Time resolved PL response of a 3% vol. DCM2:Alq_3 film to the 1.5ns pump pulse at 300K and 80K. The fits (solid lines) to the singlet exponential decay model convolved with the temporal profile of pump laser are shown.

Figure 4. (a) Edge emission spectrum at different delay times from a 3% vol. DCM2:Alq_3 film at room temperature. (b) Guest triplet absorption coefficient *vs.* wavelength after a 1μs delay.

Figure 5. Transient response of the guest triplet density *vs.* temperature in a 3% vol. DCM2:Alq_3 film following the turn-off of the pump pulse. Films of 8% and 15% vol. DCM2:Alq_3 have a similar transient response, and are omitted for clarity. The solid lines are the fits to the guest triplet decay model (Eq. (4)). Each data set is normalized to its initial value. A representative error bar of this pump probe measurement is shown. Inset: Transient response of the triplet density *vs.* temperature in an undoped Alq_3 film following a 30μs pump pulse.

Figure 6. Arrhenius plots of the triplet-triplet annihilation rate (k_{TT}) obtained for 3% (a), 8% (b), and 15% (c) vol. DCM2:Alq_3 films between T = 295K and 80K. The solid lines are the fits to models based on Marcus triplet transfer at high temperatures, and Miller-Abrahams transfer at low temperatures. The error bars correspond to the standard errors calculated from the fits.

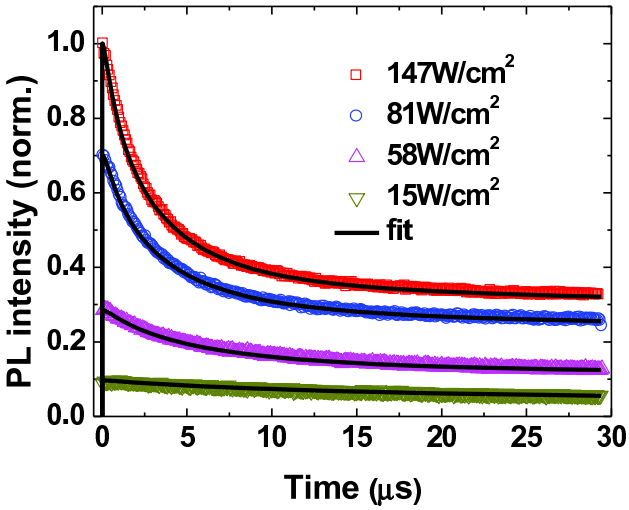
PL intensity (norm.)
Time (μs)
147W/cm2
81W/cm2
58W/cm2
15W/cm2
fit

(a)

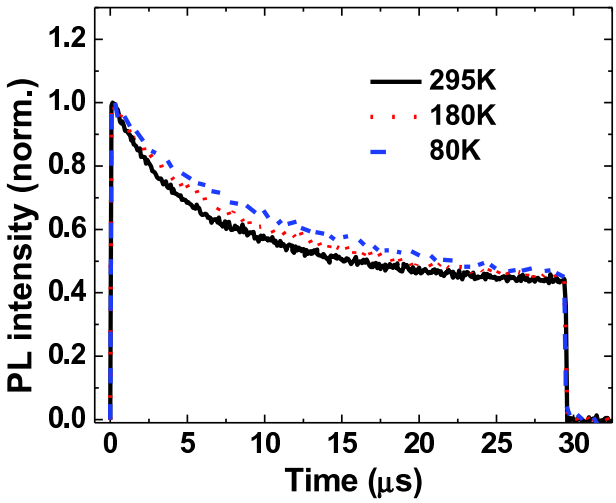
PL intensity (norm.)
Time (μs)
295K
180K
80K

(b)

Figure 1

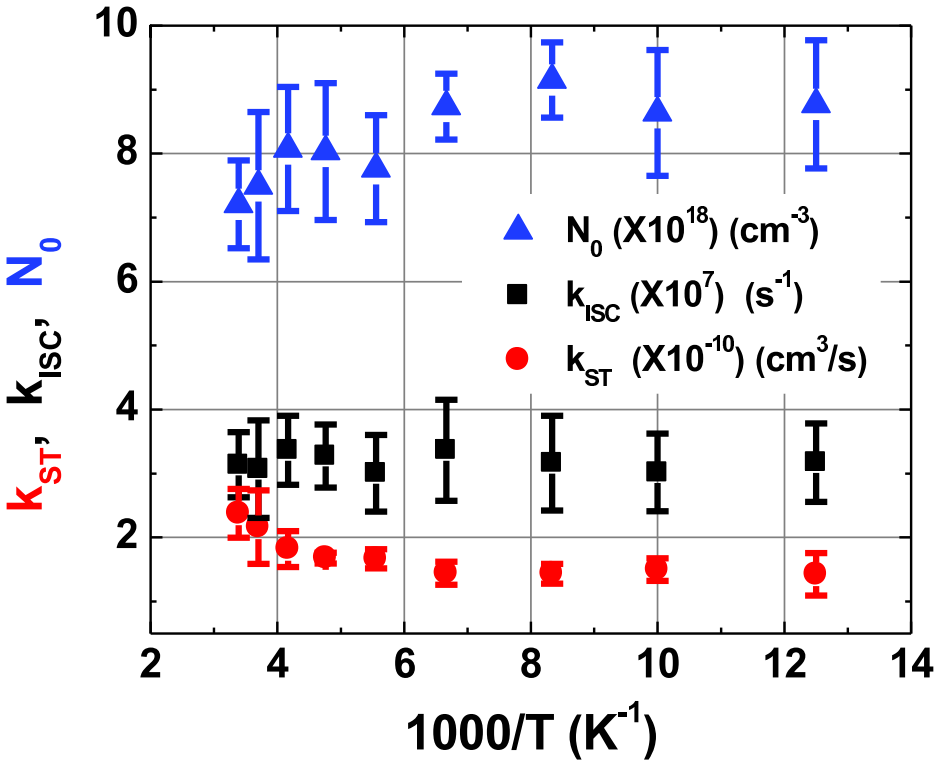
10
8
6
4
2
2
4
6
8
10
12
14
1000/T (K-1)
kST, kISC, N0
N0 (X1018) (cm-3)
kISC (X107) (s-1)
kST (X10-10) (cm3/s)

Figure 2

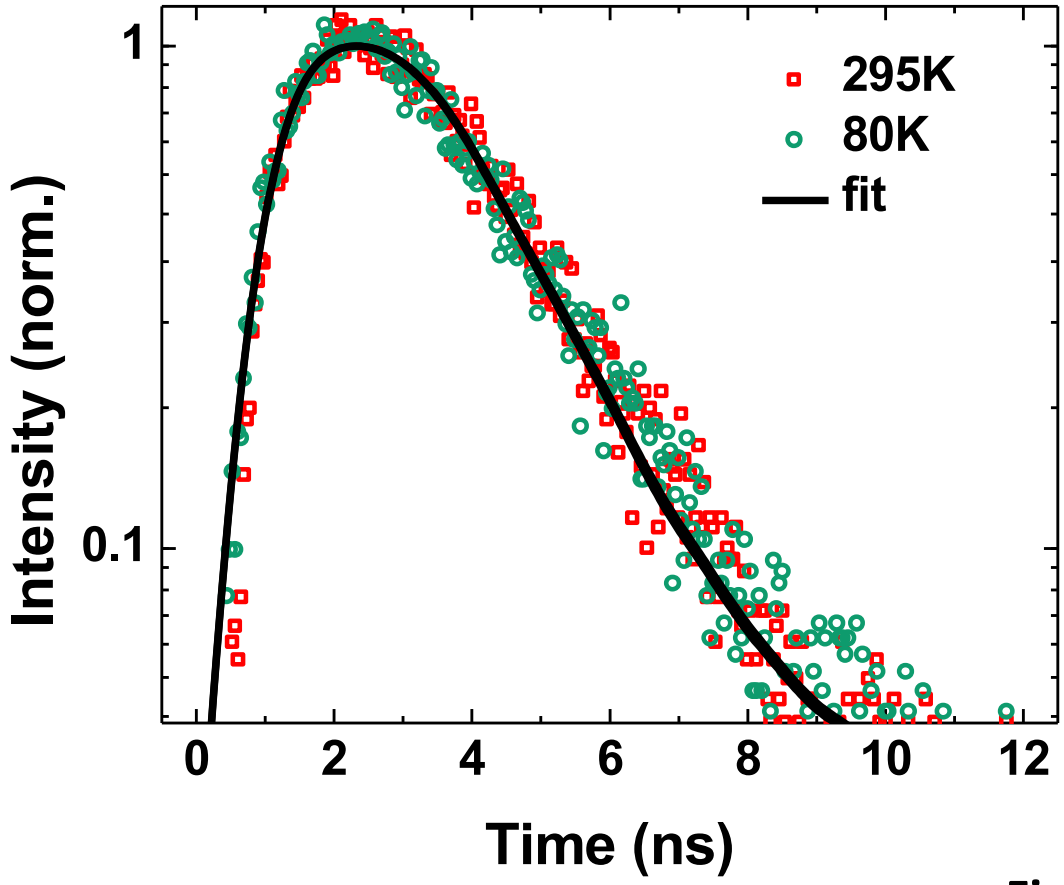

Figure 3

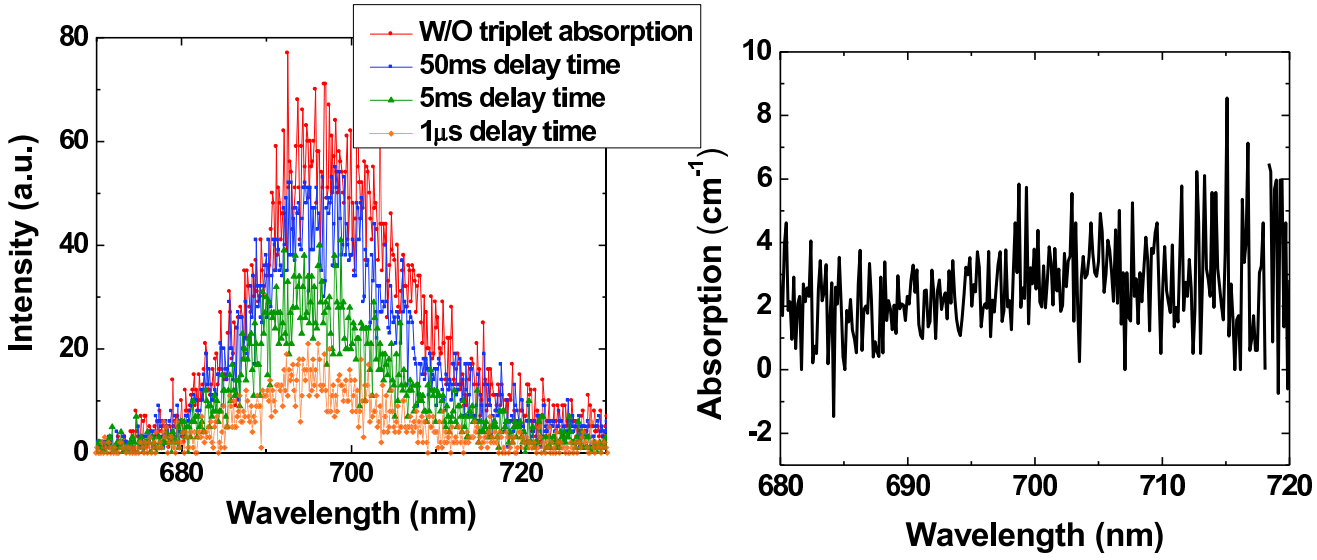
W/O triplet absorption
50ms delay time
5ms delay time
1μs delay time
Intensity (a.u.)
Wavelength (nm)
Absorption (cm-1)
Wavelength (nm)

(a) (b)

Figure 4

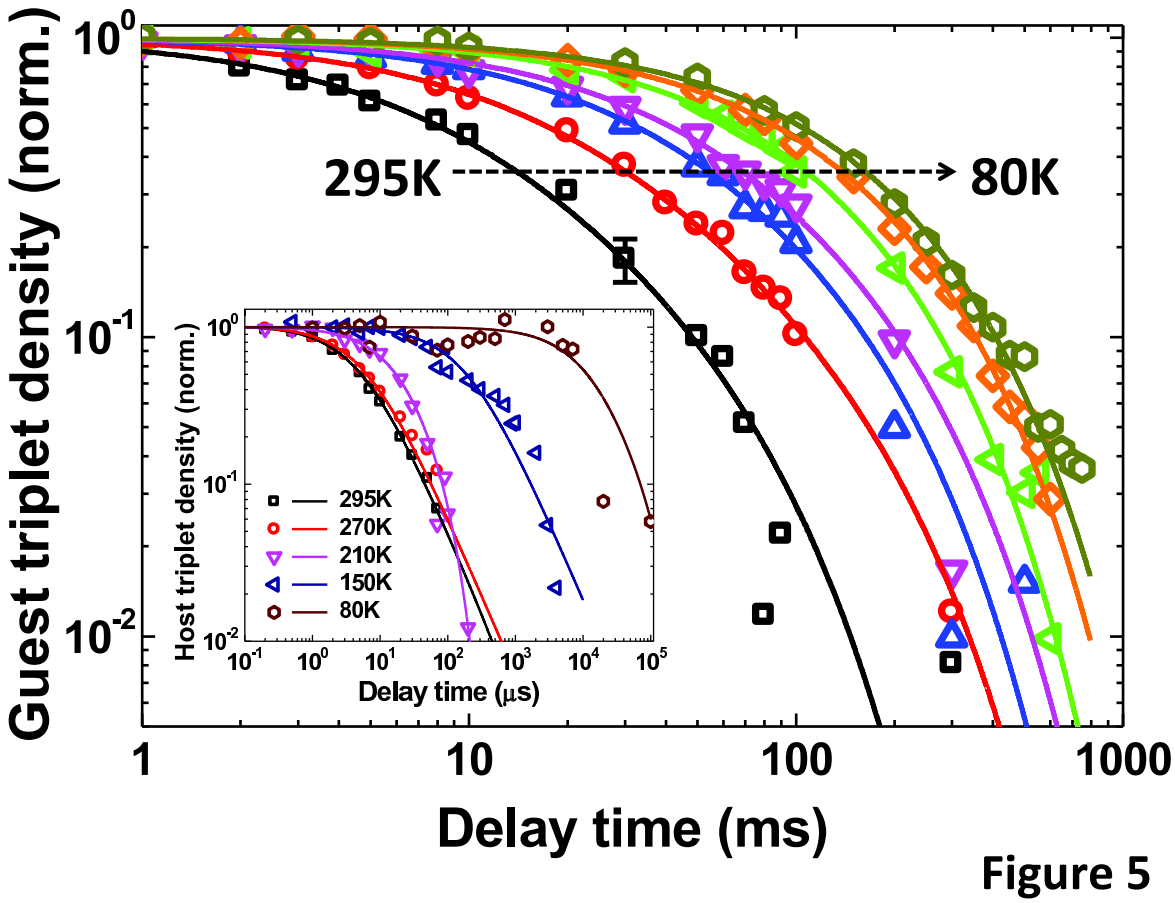
Guest triplet density (norm.)
10^0
10^-1
10^-2
295K
80K
1
10
100
1000
Delay time (ms)
Host triplet density (norm.)
295K
270K
210K
150K
80K
Delay time (μs)

Figure 5

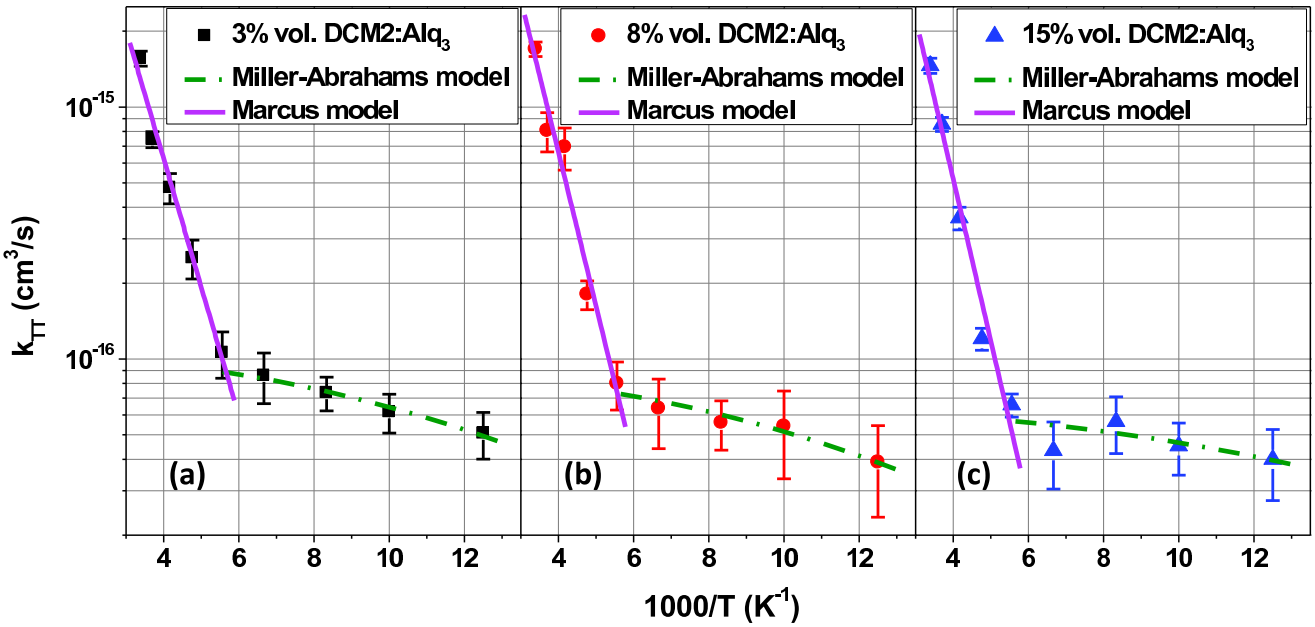
3% vol. DCM2:Alq3
Miller-Abrahams model
Marcus model
8% vol. DCM2:Alq3
Miller-Abrahams model
Marcus model
15% vol. DCM2:Alq3
Miller-Abrahams model
Marcus model
k_TT (cm^3/s)
10^-15
10^-16
(a)
(b)
(c)
4
6
8
10
12
1000/T (K^-1)

Figure 6